03

Relaxation and polarization oscillations in a wide-aperture bistable laser with a saturable absorber

© Sergey V. Fedorov, N.N. Rosanov¶, Nikolay A. Veretenov¶¶

Ioffe Institute,
194021 St. Petersburg, Russia
e-mail: sfedorov2006@bk.ru, ¶ e-mail: nnrosanov@mail.ru, ¶¶ e-mail: torrek@gmail.com

Received July 12, 2022
Revised July 12, 2022
Accepted July 26, 2022

The regions of stability of homogeneous generation regimes in a wide-aperture laser with a saturable absorber, including a semiconductor laser with a vertical output of radiation, are determined depending on the relative relaxation rate of carriers in active and passive media and on the frequency detunings of working transitions in these media with a resonant frequency of radiation, taking into account its polarization state. The excitation thresholds for relaxation and polarization oscillations are determined within the four-level model.

Keywords: wide-aperture laser, saturable absorber, relaxation and polarization oscillations

DOI: 10.21883/EOS.2022.10.54862.46-22

1. Introduction

The effect of carrier relaxation and nonzero detuning of the resonant frequency of active and passive media on the stability of scalar dissipative solitons in a bistable laser was first considered in [1]. This formulation of the problem is most relevant when searching for conditions for the implementation of dissipative solitons in micro-lasers with vertical extraction of radiation with a large aperture and with passive layers on quantum dots or wells integrated into a semiconductor micro-resonator. In the works [2,3] the possibility of realizing bistability modes in micro-lasers was considered theoretically, and in [4] — it was considered using experimental data. The polarization state of the radiation was not taken into account in this case.

In this paper, we consider the stability of generation modes that are basically homogeneous over the laser aperture in the subthreshold mode, i.e., in the hysteresis region of the homogeneous generation mode and the generationless state. Under the conditions of stability of a scalar dissipative soliton, we take into account the formation of field perturbations with different states of polarization. The uniform lasing mode can be implemented both in wide-aperture lasers and in lasers with a small aperture, for example, in semiconductor micro-lasers with one or two transverse modes (corrected for the shape of the modes). The thresholds for the onset of relaxation and polarization oscillations in a wide-aperture bistable laser are obtained analytically and numerically with a change in the resonant detuning of the active medium (alpha factor) and/or the relaxation times of two media. Comparison was made for the stability region of a homogeneous mode with the stability region of solitons with a nontrivial topology of the phase distribution or an inhomogeneous polarization state of light ([5]).

2. Model of the medium and types of relaxation oscillations

Active medium model is four-level one, the spin-flip model, [6]. The passive medium model for a saturable absorber is the two-level one. In both cases, we consider only the carrier population dynamics, assuming that the relaxation rate of dipole moments is much higher, i.e. $\gamma_{\parallel} \ll \gamma_{\perp}$, see rate equations (3.3) and (3.4) in the work[6]. In the case of a four-level model of the active medium, two radiative transitions with opposite electron spins generate photons with opposite spin directions, more precisely, we consider two photon field amplitudes with opposite circular polarization, $E_{\pm}$. The total difference between the populations of two resonant transitions is denoted by the dimensionless real amplitude N. In the absence of loss anisotropy effects, it generates oscillations only of the total intensity of the two field components $I = |E_+|^2 + |E_-|^2$. The difference between the population inversions of two transitions is denoted as n. It is related to fluctuations in the difference between the intensities of two field components $\delta I = |E_-|^2 - |E_+|^2$. The relaxation rate γ_J of the population difference n and at the same time the intensity difference δI is substantially greater than the relaxation rate of the inversion N. The values of the small parameter $\varepsilon_J = \gamma_{\parallel}/\gamma_J$ are given in [6] in the interval $1/201 \leq \varepsilon_J \leq 1/3$. In the approximation of the two-level model $\varepsilon_J \to 0$, and then it is necessary to set $n = 0$ and $\delta I = 0$ in the rate equations.

The difference between the frequencies of two transitions of the active medium and the anisotropy of the media in the resonator is neglected. As a consequence, the types of oscillations between the populations of the media and the field intensity can be divided into relaxation types (oscillations between the total population of the medium N and a

in active and passive media and the total intensity I) and polarization types (oscillations between the difference of the populations of two transitions in the active medium n and the difference between the intensities of the two radiation components δI). Further, it will be shown that with a change in the frequency detuning of the medium, the build-up of oscillations of the total field intensity with $\delta I = 0$ (relaxation oscillations in a two-level medium) is possible or, conversely, the build-up of oscillations between the amplitudes of two field components with different polarization directions $E_\pm$ with $\delta I \neq 0$, but with a constant total intensity, $I = \text{const}$. The alpha factor is denoted as the dimensionless detuning of the resonant frequency of the active or passive medium δ_g or δ_a with respect to the longitudinal mode of the resonator. The simplest way to match the resonant frequencies of the active and passive media is to choose the same medium for the saturable absorber as for the laser. In the case of a semiconductor micro-laser, it is possible to place passive and active layers (quantum wells or dots) integrated on one substrate [2,4]. The dimensionless relaxation times of the total population of carriers of two media are related to the dimensional relation $\tau_{g,a} = \kappa\gamma_\parallel^{-1}$, where κ — is the factor of linear loss of a resonator.?s specified longitudinal mode.

Next, we calculate the stability increments $\mathrm{Re}\,\lambda$ depending on the parameters of two resonant media: the relaxation time of the total intensity $\tau_{g,a}$ and $\varepsilon_J\tau_g$ of the relaxation time of the differences populations and intensities of two radiation components δI in the active medium. We consider the stability of homogeneous solutions in the wide-aperture laser model with respect to perturbations with a given spatial (transverse) scale l and wave vector $k = 2\pi/l$. Note that the characteristic size of dissipative solitons of order $l = 5{-}8$ corresponds to $k = 1$. Therefore, when estimating the instability conditions for dissipative solitons (with calibrated sizes),that for their breakup, only perturbations with $\gamma(k) > 0$ for $k > 1$ are dangerous. At the same time, homogeneous perturbations with $k = 0$ also violate the stability of localized states, since they lead to temporal oscillations of the soliton amplitude, which are uniform along the distribution coordinate. For a dissipative soliton, such oscillations with sufficiently large amplitude can lead to the breakdown into a generationless state if the intensity oscillation amplitude is greater than the difference between the intensities of the upper and intermediate branches of the hysteresis.

3. Equations for field and populations

In the quasi-optical and mean-field approximations, the vector field envelope of the electric strength $\mathbf{E} = E_x, E_y$ is related to the total strength $\tilde{\mathbf{E}}$ by the relation $\tilde{\mathbf{E}} = 2\,\mathrm{Re}[\mathbf{E}(x, y, t)e^{ik_0 z - i\omega_0 t}]$, where z is coordinate along the resonator axis, x and y are transverse Cartesian coordinates, t is time, ω_0 is carrier frequency and k_0 is corresponding wavenumber. It is also convenient to use the left and right circular polarization components $E_\pm = \frac{1}{\sqrt{2}}(E_x \pm iE_y)$. The amplitudes of the envelope are complex and the intensity of the circular components is expressed in terms of the Stokes parameters s_i, see [7]:

$$I = |E_+|^2 + |E_-|^2 = s_0, \quad \Delta I = |E_-|^2 - |E_+|^2 = s_3. \quad (1)$$

In the regions of the soliton, where $\delta I = s_3 = 0$, the is linear light polarization, otherwise is- elliptical one or circular one.

In dimensionless form, the equations for the field and populations are as follows:

$$\partial_t E_\pm - (i + d)\nabla_\perp^2 E_\pm = \big[-1 - (1 - i\delta_a)a + (1 - i\delta_g)(N \pm n)\big]E_\pm, \quad (2)$$

$$\tau_g\partial_t N = -(1 + b_g I)(N - N_s) + b_g\delta I(n - n_s),$$
$$\tau_g\partial_t n = -(1/\varepsilon_J + b_g I)(n - n_s) + b_g\delta I(N - N_s),$$
$$\tau_a\partial_t a = -(1 + b_a I)(a - a_s). \quad (3)$$

These equations, unlike [6], take into account the population dynamics of a passive medium (absorber) with a two-level model (a is inverse population normalized to linear losses), and unlike [6,8] The loss angular selectivity factor d is introduced into the equation for the field. In relaxation equations (3), the following notation is used for the steady-state populations of two media as functions of the intensities:

$$N_s(I, \delta I) = \frac{N_0}{1 + b_g I - \frac{\varepsilon_J b_g^2 \delta I^2}{1 + \varepsilon_J b_g I}},$$

$$n_s(I, \delta I) = \frac{\varepsilon_J b_g \delta I}{1 + \varepsilon_J b_g I} N_s(I, \delta I), \quad a_s(I) = \frac{a_0}{1 + b_a I}. \quad (4)$$

In the inertialess approximation, the dimensionless relaxation times are $\tau_{g,a} \to 0$. The value of the dimensionless saturation factor b_g is determined by the choice of normalization of the field amplitude $E_\pm$. In accordance with (4), we use normalization with unit saturation intensity of the absorber, $b_a = 1$. The dimensionless time in (2) and (3) is normalized to unit linear losses: $t = \kappa\tilde{t}$. In contrast to [8], here we do not take into account the loss anisotropy of two cavity modes with a given linear polarization and assume that the resonant frequencies of two modes with orthogonal polarizations coincide.

4. Stability of homogeneous solutions

Solving equations (2) and (3) in the homogeneous case, we necessarily obtain the case of linear polarization $\delta I = s_3 = 0$ for the four-level model, when $\varepsilon_J \neq 0$. Solution with a single circular polarization, when the amplitude of the other component is zero, is always unstable for $\varepsilon_J \neq 0$ [5]. For $\varepsilon_J = 0$, the equations of the medium and the field without anisotropy are degenerate with respect to the polarization state, i.e., then, any homogeneous polarization states can be realized. Ignoring the anisotropy of media, let's consider the instability of only a linearly polarized field, $|E_\pm| = |E_s|$.

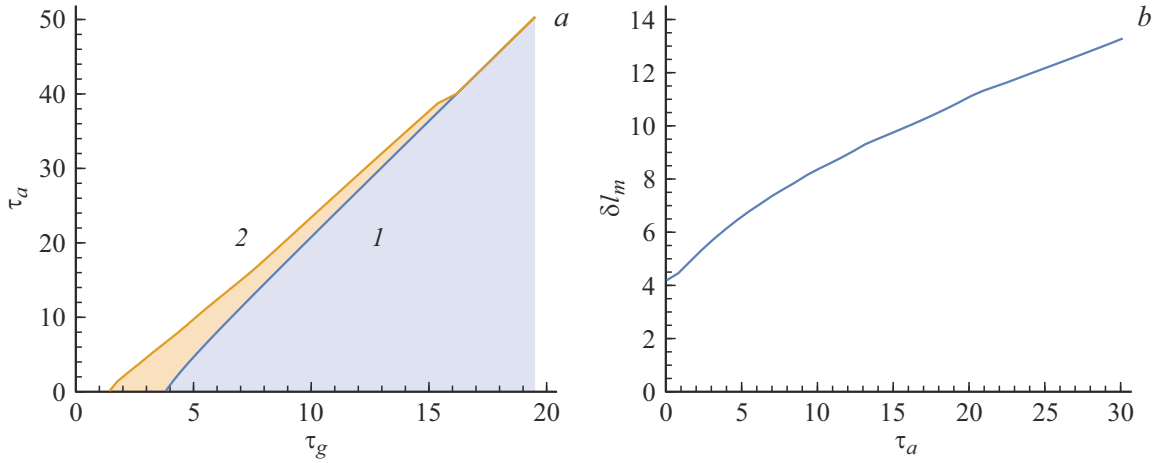

Figure 1. Boundaries of the region of instability with respect to homogeneous perturbations (*1*, Andronov–Hopf bifurcation, the region to the right of the curve) and the region of small-scale instability (to the right of the curve) *2*, including the region *1*) on planes of dimensionless relaxation times (τ_g, τ_a). The diagram (*b*) shows the value of the most dangerous instability scale δl_m. $\delta k_{\max} = 2\pi/\delta L_m$, depending on the relaxation time of the passive medium τ_a, for which the growth increment reaches a maximum, and the value of the relaxation time of the active medium $\tau_g(\tau_a)$ corresponds to the boundary of the small-scale instability region, curve *2*.

Small-scale instability of homogeneous or localized solutions appears only in wide-aperture lasers. For lasers with a small aperture, the perturbations can be considered as uniform. Let's substitute into (2), (3) the perturbed homogeneous solution: $E_\pm \cong (E_s + F_\pm)e^{i\nu t}$, $a \cong a_s + \delta a$, $N \cong N_s + \delta N$, $n \cong \delta n$. Here $F_\pm$ is the amplitude of perturbations of the circular components. The resulting linear equations are divided into equations for the amplitudes of relaxation, $F = F_+ + F_-$, and polarization, $R = F_+ - F_-$, perturbations. From them it is not difficult to obtain algebraic equations for the oscillation amplitude:

$$F(t) \cong A_P e^{\lambda t} + B_p^* e^{\lambda^* t}, \quad R(t) \cong A_m e^{\lambda t} + B_m^* e^{\lambda^* t},$$

$$\delta a(t) \cong q e^{\lambda t} + q^* e^{\lambda^* t}, \quad \begin{cases} \delta N(t) \cong p e^{\lambda t} + p^* e^{\lambda^* t}, \\ \delta n(t) \cong \eta e^{\lambda t} + \eta^* e^{\lambda^* t}. \end{cases} \tag{5}$$

The solvability condition of the latter, firstly, is the cubic equation for the growth rate of perturbations λ:

$$\tau_g \tau_a \lambda^3 + (\tau_g b_{as} + \tau_a b_{gs})\lambda^2 + \big[b_{gs} b_{as} + 2(\tau_a N_s b_g - \tau_g a_s b_a) I_s\big]\lambda + 2(b_{as} N_s b_g - b_{gs} a_s b_a) I_s = 0 \tag{6}$$

for relaxation oscillations, where $b_{as,gs} = 1 + b_{a,g} I_s$ and I_s is total intensity of the unperturbed mode. Secondly, for polarization oscillations we obtain a quadratic equation:

$$\tau_g \lambda^2 + \lambda(1/\varepsilon_J + b_g I_s) + 2 b_g N_s I_s = 0. \tag{7}$$

Solution (7) always gives $\mathrm{Re}\,\lambda_\pm < 0$, i.e., there is no Andronov–Hopf bifurcation for polarization oscillations and perturbations with constant total intensity and $\delta I \neq 0$ is always damped. For

$$\tau_g < \frac{1}{8 b_g N_s I_s} (1/\varepsilon_J + b_g I_s)^2$$

the oscillation in damped oscillatory modes of motion they are missing because $\mathrm{Im}\,\lambda_\pm = 0$ In the inertialess limit $\varepsilon_J \to 0$, the population difference n does not oscillate or accompanies the relaxation oscillations of the population sum. The regions of instability of relaxation oscillations (the Andronov–Hopf bifurcation) are shown in Fig. 1.

Next, we consider the small-scale instability of a homogeneous or soliton solution. We substitute the perturbed amplitudes into (2) and obtain linearized equations with coefficients depending on the coordinates, which are expressed through the soliton amplitude $E_{\pm s}$. Stationary solution (3) $E_\pm = E_{\pm s}(x, y)e^{i\nu t}$ taking into account (4) $(a = a_s, N = N_s, n = n_s)$ is determined by the equations:

$$(i + d)\nabla_\perp^2 E_{\pm s} - (1 + i\nu)E_{\pm s} - (1 - i\delta_a)a_s E_{\pm s} + (1 - i\delta_g)(N_s \pm n_s)E_{\pm s} = 0. \tag{8}$$

The equations for perturbed amplitudes, which are also valid for soliton perturbations, $F_\pm(x, y, t)$

$$E_\pm \cong E_{\pm s}(x, y)e^{i\nu t} + F_\pm e^{i\nu t}, \quad \begin{matrix} N \cong N_s(x, y) + \delta N \\ a \cong a_s(x, y)\delta a \end{matrix}, \quad n \cong \delta n \tag{9}$$

are putting down separately for relaxation $F = F_+ + F_-$ and polarization $R = F_+ - F_-$ perturbations. Next, we substitute the perturbation amplitudes with a given scale $|\mathbf{k}|$ and growth increment λ:

$$F \cong A_p e^{\lambda t + i\mathbf{kr}} + B_p^* e^{\lambda^* t - i\mathbf{kr}}, \quad R \cong A_m e^{\lambda t + i\mathbf{kr}} + B_m^* e^{\lambda^* t - i\mathbf{kr}},$$

$$\delta a \cong q e^{\lambda t + i\mathbf{kr}} + q^* e^{\lambda^* t - i\mathbf{kr}}, \quad \begin{cases} \delta N \cong p e^{\lambda t + i\mathbf{kr}} + p^* e^{\lambda^* t - i\mathbf{kr}}, \\ \delta N \cong \eta e^{\lambda t + i\mathbf{kr}} + \eta^* e^{\lambda^* t - i\mathbf{kr}}. \end{cases} \tag{10}$$

For homogeneous solution $I_s = \mathrm{const}$, and linear equations on $A_{p,m} B_{p,m}$, p, η become algebraic. The condition for

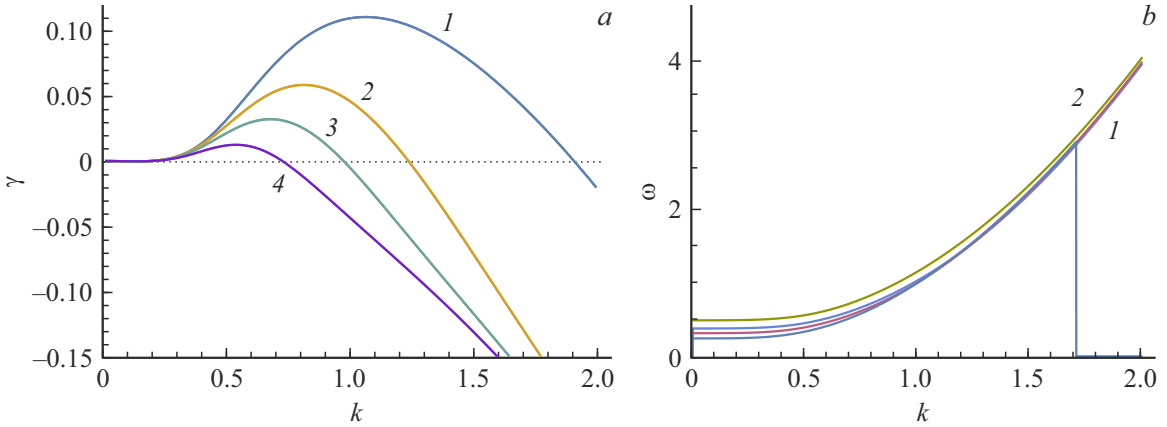

Figure 2. Dependences (a) of the growth increment of small-scale perturbations $\lambda = \gamma + i\omega$ on the boundary of the Andronov–Hopf bifurcation region (curve *1* in Fig. 1) and (b) frequency of time oscillations on the wave number; almost does not depend on the scale of perturbations in the region of their instability (curves *1, 2* for two frequencies). The values of the relaxation times $\tau_a = 0$, $\tau_g = 3.79$ (curve *1*), $\tau_a = 5$, $\tau_g = 5.1$ (*2*), $\tau_a - 10$, $\tau_g = 6.61$ (*3*), $\tau_a = 20$, $\tau_g = 9.77$ (*4*).

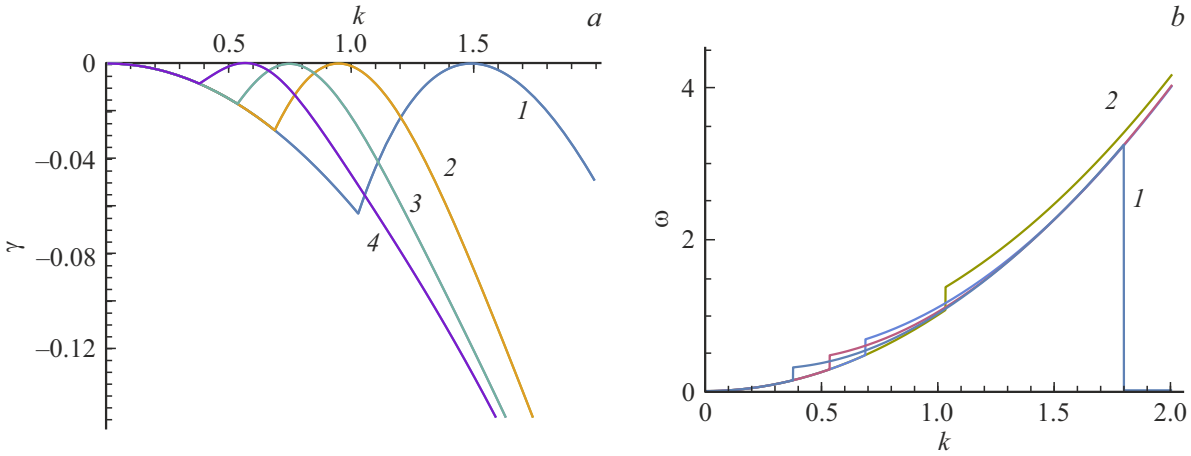

Figure 3. Dependences (a) of the growth increment of small-scale disturbances at the boundary of the small-scale instability region (curve *2* in Fig. 1) and (b) frequencies temporal oscillations of ω from the wave number. The values of the relaxation times $\tau_a = 0$, $\tau_g = 1.4$ (curve *1*), $\tau_a = 5$, $\tau_g = 3.18$ (*2*), $\tau_a - 10$, $\tau_g = 5.12$ (*3*), $\tau_a = 20$, $\tau_g = 8.84$ (*4*).

their solvability are equations for the growth increment of the sixth degree by λ for relaxation perturbations. For polarization oscillations with amplitude R, it separates and becomes a third-degree equation:

$$\tau_g \lambda \lambda_{kk}^2 + (1/\varepsilon_J + b_g I_s)\lambda_{kk}^2 + 2N_s b_g I_s(\lambda_k - \delta_g k^2) = 0, \tag{11}$$

where

$$\lambda_k = \lambda + dk^2, \quad \lambda_{kk}^2 = \lambda_k^2 + k^4 = (\lambda + dk^2)^2 + k^4,$$

and for $k = 0$ to (7) in (11) the solution $\lambda = 0$ is added. It is this branch of solutions, which tend to zero for $k \to 0$, that generates the small-scale instability of polarization perturbations. The expansion (11) for small values of $k^2 \ll 1$ gives two solutions with increment close to zero: $\lambda(k^2) \cong \lambda_{\pm\delta} + \lambda_{\pm 1}k^2$ for $\delta_g > 0$, and for $\delta_g < 0$ respectively:

$$\lambda_{+1} = \delta_g - d \text{ and } \lambda_{+\delta} = 0, \text{ or } \lambda_{-1} = -4(\delta_g + d)N_s b_g I_s \tau_g \varepsilon_{Js}^2 c_1$$

$$\text{and} \quad \lambda_{-\delta} \cong -2N_{gs} < 0, \quad \varepsilon_{Js} = \frac{\varepsilon_J}{1 + b_g I_s \varepsilon_J}.$$

Only the first of them in the first order of smallness in k^2 gives a positive growth increment. The increment maximum is reached at $k = k_{\max}$, besides $k_{\max} = 0$ for $\delta_g < d$ and

$$k_{\max}^2 = \varepsilon_{Js} N_s b_g I_s \frac{\delta_g - d}{1 + \delta_g^2} > 0, \text{ for } \delta_g > d. \tag{12}$$

Finally, the maximum increment is given by:

$$\lambda_{\max} = \frac{1}{2}\varepsilon_{Js} N_s b_g I_s \frac{(\delta_g - d)^2}{1 + \delta_g^2}. \tag{13}$$

Of interest is only the case of positive values of detunings, when $\lambda(0) = 0$, $\lambda_{\max} > 0$, and since the last relation makes sense only under the condition $k_{\max}^2 \sim \delta_g - d > 0$, then the polarization oscillations for small values of $k_{\max}^2$ do not

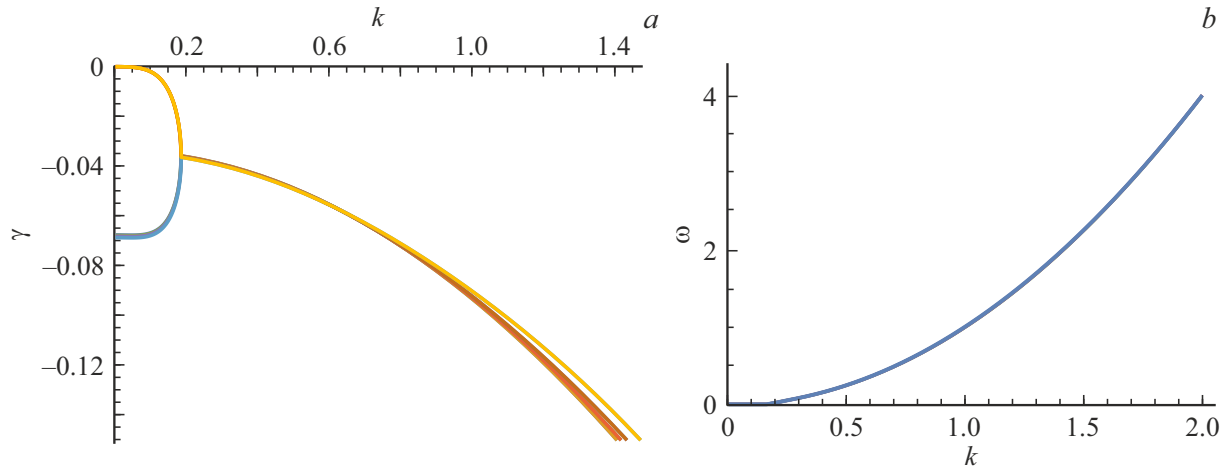

Figure 4. Dependences (a) of the increment of decrease in polarization oscillations for selected values of relaxation times at the boundary of the region of small-scale instability of relaxation oscillations (curve *2* in Fig. 1) and (b) frequency of temporal oscillations ω on the wavenumber. The values of the relaxation times are the same as in Fig. 3, but in accordance with (10) and (12), the increment of polarization oscillations does not depend on τ_a and weakly depends on τ_g; $\delta_g = \delta_a = 0$, $d = 0.06$.

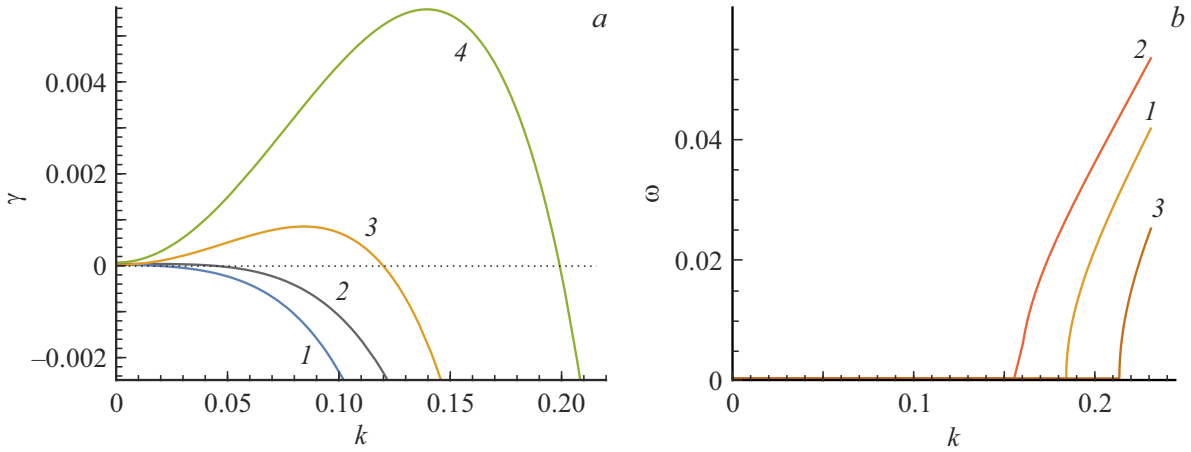

Figure 5. Dependences (a) of the growth increment of polarization oscillations for three values of the alpha factor in the region of small-scale instability of the uniform generation regime and (b) the frequency of time oscillations $\omega(k)$ i.e.curves *1, 2, 3* for three frequencies in the right figure from the wave number $\delta_g = 0$ (curve *1*), -0.3 (*2*), 0.3 (*3*). The absorber is resonantly tuned, $\delta_a = 0$. The increment of polarization oscillations does not depend on the relaxation time τ_a, but $\tau_g = 5$; $d = 0.06$.

decay only for $\delta_g > d$, i.e., only for positive values of the alpha factor.

It is possible to derive an expression for the growth threshold of relaxation oscillations, which is valid, as in the case of polarization oscillations (12), for small values of $k^2 \ll 1$. The increment equation for relaxation oscillations already has six roots, three of which degenerate for homogeneous perturbations, $\lambda(0) = 0$:

$$\begin{aligned}&\left[(\tau_a\lambda + b_{as})(\lambda_k^2 + k^4) - 2a_s b_a I_s(\lambda_k - \delta_a k^2)\right]\\ &\times\left[(\tau_g\lambda + b_{gs})(\lambda_k^2 + k^4) + 2N_s b_g I_s(\lambda_k - \delta_g k^2)\right]\\ &+ 4a_s N_s b_a b_g I_s^2(\lambda_k - \delta_g k^2)(\lambda_k - \delta_a k^2) = 0, \qquad (14)\end{aligned}$$

where $\lambda_k = \lambda(k^2) + dk^2$ and $\delta_{dg,da} = \delta_{g,a} - d$. Substitution into (14) $\lambda_k \cong (\lambda_1 + d)k^2 + \lambda_2 k^4$ gives the solution

$$\lambda_1 \cong \frac{\delta_{dg} - b_{gas}\delta_{da}}{1 - b_{gas}}, \quad b_{gas} = \frac{b_{gs}N_{as}}{b_{as}N_{gs}}.$$

Thus, at $k \to 0$, $\lambda(k^2) \to 0$ the growth increment of relaxation oscillations is $\lambda > 0$ if $\lambda'(0) = \lambda_1 > 0$:

$$\delta_g > d + b_{gas}(\delta_a - d),$$

$$b_{gas} = \frac{(1 + b_g I_s)^2 b_a a_0}{(1 + b_a I_s)^2 b_g g_0} < 1. \qquad (15)$$

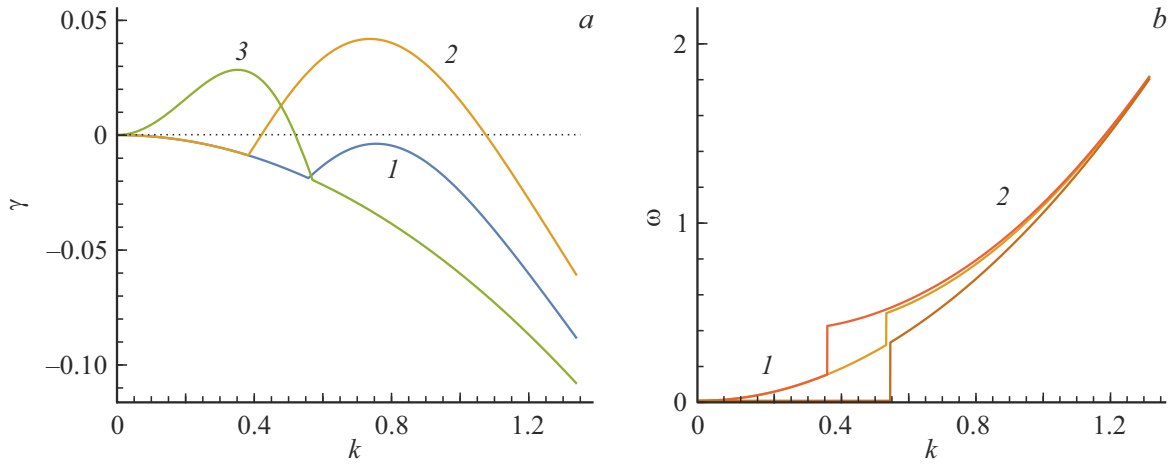

Figure 6. Dependences (a) of the increase increment of relaxation oscillations for three values of the alpha factor in the region of small-scale instability of the uniform generation regime: $\delta_g = 0$ (curve *1*), 0.3 (*2*), -0.3 (*3*) and (b) time oscillation frequencies $\omega(k)$ — curves *1, 2* for two frequencies from the wavenumber. $\delta_a = 0$. The values of the relaxation times $\tau_1 = 10$, $\tau_g = 5$; $d = 0.06$.

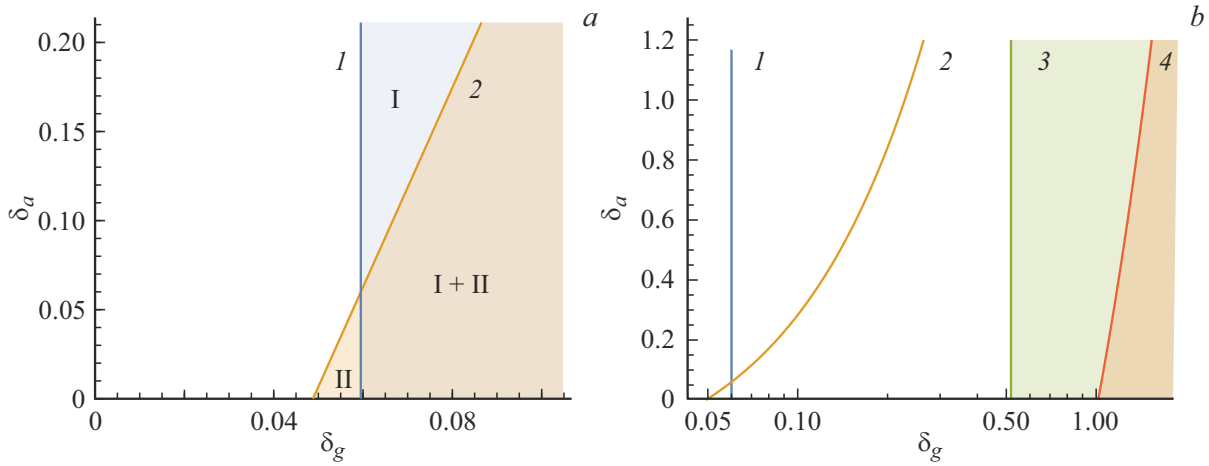

Figure 7. Boundaries of the region of instability with respect to homogeneous perturbations on the detuning plane, (δ_g, δ_a), in linear (a) and semilogarithmic (b) scales. Region I is region of instability of polarization oscillations The region boundary (curve *1*, Andronov–Hopf bifurcation) corresponds to the threshold condition (12). In the part of the region, to the left of the curve *2*, the polarization perturbations increase (instability), while the relaxation perturbations decrease. In the region II of the region of small-scale instability of relaxation perturbations to the left of the curve *1* i.e. polarization perturbations decrease, while relaxation perturbations increase. The boundary of the region *2* corresponds to the threshold condition (15). In the figure (b), the estimated regions of soliton instability with a characteristic scale $k = 1$ are additionally shaded. Curve *3* is for the region of small-scale instability due to polarization oscillations, curve *4* is for relaxation oscillations; $g_0 = 2.117$, $\tau_g = 5$, $\tau_a = 10$.

5. Calculation of dependences of growth increments of perturbations

Using the solution of equations (11), (14), we present here a pattern of the stability of polarization and relaxation oscillations, taking into account their dependence on the spatial scale $k = |\mathbf{k}|$. First, we consider the case of zero values of the alpha factor, $\delta_g = \delta_a = 0$. Figure 1 shows the regions of instability of the homogeneous solution E_s for homogeneous perturbations $k = 0$, curve *1*, and for small-scale instability, curve *2*. The region of existence of the latter under conditions of stability of homogeneous perturbations is adjacent to the region *1*. The calculations were carried out for the most characteristic value of the control parameter i.e. gain ratio $g_0 = 2.114$, for which the stability regions of polarization solitons are calculated: $a_0 = 2$, $b_g = 0.1$, $b_a = 1$, $d = 0.06$. Figure 2 shows the calculation of the complex growth rate of small-scale perturbations, $\lambda(k) = \gamma(k) + i\omega(k)$, from their scale for several points of the boundary of the region of instability of homogeneous perturbations. It can be seen that as the relaxation time increases, the maximum value of the increment decreases, as does the width of the perturbation spectrum, passing to a region with predominantly Andronov–Hopf instability,

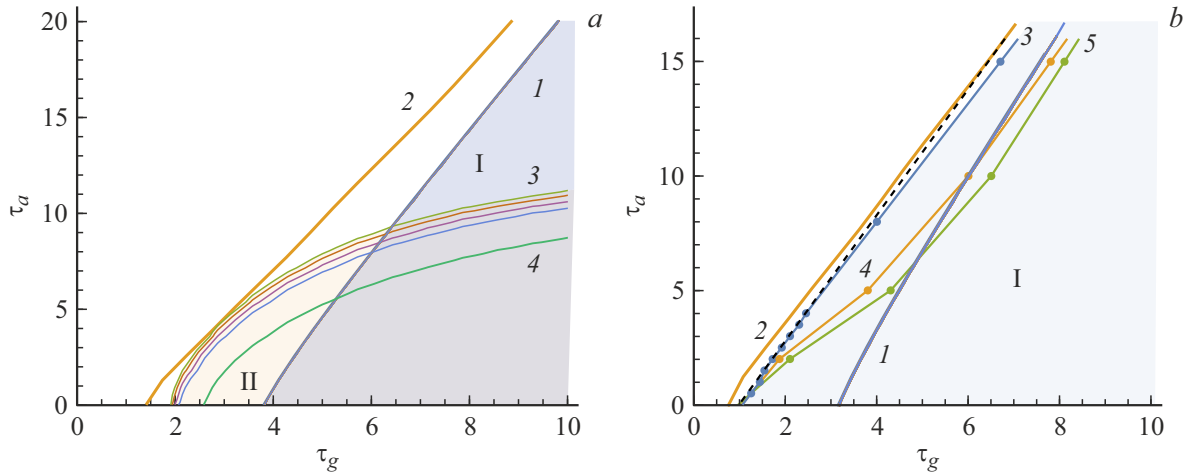

Figure 8. Regions of instability of relaxation oscillations with respect to homogeneous perturbations (region I to the right of the curve *1* is region of Andronov–Hopf instability) and regions of small-scale instability II (to the right of the curve *2*, including the region *1*) on the plane of dimensionless relaxation times (τ_g, τ_a). The regions of soliton instability with a characteristic scale $k = 1$ are additionally shaded for different values of the alpha factor $\delta_g = 0$ (to the right of the curve *3*), 0.025, 0.06, 0.1, 0.3 (*4*). $\delta_a = 0$, $g_0 = 2.117$. On the (b) diagram, the *1* and *2* curves correspond to the uniform regime, as well as on the (a) graph, the dashed curve is the boundary of the stability region of a scalar soliton with $m = 1$ and $\eta = 0$. Curve *3* is boundary of the region of stability of a polarization soliton with unit charge Poincar? $\eta = 1$ Curve *4* is for $\eta = 2$ and curve *5* is for $\eta = 3$. Alpha factor $\delta_g = 0$.

once the two boundaries of the regions in Fig. 1,are merging. Finally, Fig. 3 shows the dependences of increments on the scale at the boundary of the small-scale instability (curve *2* in Fig. 1).

Figure 4 shows the dependences of the decrease increment of polarization oscillations for zero values of the alpha factor.

Now let's consider the polarization and relaxation oscillations for the alpha factor above the threshold value, see (14). Figure 5 shows the dependences of the decrease and increase increments of polarization oscillations for values of the alpha factor $\delta_g = 0.3$ $(\delta_g > d)$ and $\delta_g = -0.3$ $(\delta_g < -d)$.

It can be seen that, with respect to relaxation oscillations, the homogeneous generation mode is unstable only for positive values of the alpha factor, $\delta_g > d$, and the maximum increase increment is reached for sufficiently long-wavelength perturbations, $\delta l_m \sim 50-100$, $k_{\max} = 2\pi/\delta l_m$, i.e., by order of magnitude greater than the characteristic width of the soliton. Perturbations with such a scale increase mostly without temporal oscillations. Polarization oscillations at negative values of the alpha factor (resonance detuning) are damped. Homogeneous perturbations, $k = 0$, are always neutrally stable, $\gamma = 0$.

Figure 6 shows the increase increments of relaxation oscillations for the same conditions as in Fig. 5. It can be seen that at sufficiently large values of the alpha factor relaxation oscillations also increase (instability), and for both values of the sign of the resonant detuning δ_g.

Figure 7 shows the regions of instability with respect to the increase of polarization and relaxation oscillations on the plane of resonant detunings, (δ_g, δ_a). The regions of instability are given by the threshold conditions (12), $\delta_g > d$, and (15), $\delta_d > d + b_{gas}(\delta_a - d)$, respectively. The threshold conditions do not depend on the relaxation times in the $0 < k^2_{\max} \ll 1$ approximation, which is observed for the chosen parameters. This means that an increase in detuning δ_g leads to the development of instability for all values $\tau_{g,a}$ at once. However, for dissipative solitons with a calibrated width, the stability regions increase significantly, see curves *3* and *4* in Figs 7 and 8. On the right side of Fig. 7 and Fig. 8, the regions of small-scale instability of solitons are shown, the position estimate of which is given by the positive increment $\gamma(k) > 0$ for $k = 1$.

Fig. 8, *a* shows the regions of instability of relaxation perturbations of the homogeneous solution (7) for homogeneous perturbations ($k = 0$, curve *1*) and for small-scale instability (curve *2*) corresponding to Fig. 1. Estimated areas of small-scale instability of harmonics with a characteristic scale $k = 1$ for relaxation oscillations and for different values of the alpha factor, are additionally shaded. They are given by the condition $\gamma(k) > 0$ for $k = 1$. It can be seen that the small-scale instability with a large wavelength, $k = 1$ (curves *3, 4*), affects the stability of a homogeneous mode or soliton much less than long-wave harmonics with $k \to 0$, if the absorber relaxation time is large enough, $\tau_a > 10$, and even for sufficiently large alpha factors, up to $\delta_g > 1-2$. In the second diagram, Fig. 8, *b* are shown to compare the boundaries of the instability regions of the homogeneous regime (curves *1* and *2* for homogeneous and small-scale disturbances, as in the figure on the left) with the boundaries regions of instability of vector solitons with different Poincar? charge η [5] (Poincar? charge is understood as the number

of revolutions of the main axis of the polarization ellipse when going around the polarization singularity point along a closed contour). It can be seen that the boundary of the region of instability of the scalar soliton (with charge $\eta = 0$) almost coincides with the boundary of the region of small-scale instability of the homogeneous generation regime, and in the region of instability under homogeneous perturbations, which can be realized for lasers with a small aperture, the polarization solitons with a large Poincar? charge.

Conclusion

The stability thresholds for polarization and relaxation oscillations in lasers with saturable absorption are determined within the framework of a four-level model of the active medium, taking into account the polarization of radiation. It is shown that, at small values of the alpha factor, the instability can be compensated by passing to localized modes (vector solitons), which is most significant for large relaxation times of the active medium. The regions of stability due to both types of oscillations are determined, and it is shown that polarization oscillations of the medium can also develop in wide-aperture lasers, i.e., oscillations at which the total intensity is almost constant, and the difference between the intensities of the circular components of the radiation oscillates with increasing amplitude. Increasing the relaxation time and alpha factor of the absorber relative to the values of these quantities for the active medium increases the region of stability of the uniform generation mode (Figs 7 and 8). The same applies to localized generation modes (solitons) (Fig. 8).

Funding

The study supported by RSF grant 18-12-00075.

Conflict of interest

The authors declare that they have no conflict of interest.

References

[1] S.V. Fedorov, A.G. Vladimirov, N.N. Rosanov, G.V. Khodova. Phys. Rev. E, **61** (5), 5814 (2000). DOI: 10.1103/PhysRevE.61.5814
[2] S.V. Fedorov. Opt. Spectr.**106** (4), 633 (2009). [S.V. Fedorov. Opt. Spectr., **106** (4), 564 (2009). DOI: 10.1134/S0030400X09040183].
[3] S.V. Fedorov, S.A. Blokhin, L.Ya. Karachinsky. Opt. Spectr. **109** (2), 324 (2010). [S.V. Fedorov, S.A. Blokhin, L.Ya. Karachinskii. Opt. Spectr., **109** (2), 290 (2010). DOI: 10.1134/S0030400X10080230].
[4] S.V. Fedorov, S.A. Blokhin, L.Ya. Karachinsky. Opt. Spectr., **111** (1), 153 (2011). [S.V. Fedorov, S.A. Blokhin, L.Ya. Karachinskii. Opt. Spectr., **111** (1), 142 (2011). DOI: 10.1134/S0030400X1107006X].
[5] N.A. Veretenov, S.V. Fedorov, N.N. Rosanov. Phys. Rev. Lett., (2022). Submitted.
[6] M. San Miguel, Q. Feng, J.V. Moloney. Phys. Rev. A., **52** (2), 1728 (1995). DOI: 10.1103/PhysRevA.52.1728.
[7] M.V. Berry, M.R. Dennis. Proc. R. Soc. London A, **457** (2005), 141 (2001). DOI: 10.1098/rspa.2000.0660.
[8] K. Panajotov, M. Tlidi. Opt. Lett., **43** (22), 5663 (2018). DOI: 10.1364/OL.43.005663.